

An Approach for Actuator Controlled Motion of Peripheral Milling Tools on Wood

Christian Gottlöber*, Klaus Röbenack**, Danish Ahmed** and Stephan Eckhardt**

*(Institute of Wood and Paper Technology, Technische Universität Dresden, Dresden, Germany)

** (Institute of Control Theory, Technische Universität Dresden, Dresden, Germany)

ABSTARCT

Peripheral milling is a very important procedure in terms of work piece shaping by cutting in wood industry. Because of the kinematic principle of this procedure a more or less wavy structure on the cutting area of the work piece appears, the so called cutter marks. That is why in many cases after cutting, expensive extra finishing procedures like sanding must be applied to smoothen the work piece surface. An approach to improve this situation is given by an actuator controlled motion of the tool spindle position to realize a linear cutting motion during the edge approach to the work piece. A control strategy was created and first experiments with a test setup using magnetic bearings have been done successfully.

Keywords - active magnetic bearing, cutter-marks, flatness based control, peripheral milling

I. INTRODUCTION

Wood cutting procedures with differences between the cutting and the feeding direction generate specific, regular kinematic patterns on the work piece surface. Generally this happens during peripheral milling (Fig. 1). The obtained wavy structure of the cutting area on the work piece is called cutter-marks and belongs to the kinematical roughness and waviness. The periodical shape of the surface cannot be avoided completely without actuator controlled motion and is given by the kinematical principle of the peripheral milling operation [1, 2]. The only way to minimise these cutter-marks is to work with very precise adjusted tool edges and optimal kinematic cutting conditions (high tool revolution frequency, moderate feed speed, big number of tool edges).

After peripheral milling some finishing procedures like smoothing or sanding are necessary to obtain a flat surface without strong topographical differences on the work piece surface finally. Therefore, there is an extra economical effort necessary.

Basically the topography of the cutter-marks on the work piece results due to the relationship between the tool and work piece motion and can be

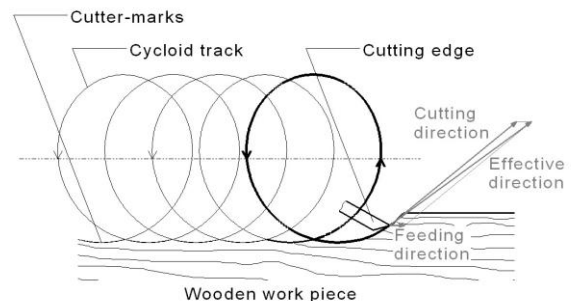


Figure 1. Development of cutter-marks because of the cycloid track of cutting edge when peripheral milling of wood.

described as part of a regular periodic trajectory of a prolonged cycloid (Fig. 1). Additionally there are displacements because of adjustment and wear failures at the cutting edges as well as disturbance vibrations inside the machine caused by specific machine construction, process forces and imbalances. Finally the surface topography of the machined area on a wooden work piece results from all influences mentioned before.

II. IDEA

To improve this limited situation the kinematical relation must be influenced dynamically. Based on an idea of the Institute of Wood and Paper Technology and experiences of the Laboratory of Control Theory, both of the Technische Universität Dresden, a new positioning mechanism on the tool bearings will be developed to reduce the cutter-marks and improve the quality of the milling process on wood. The approach uses a correction of the trajectory of the tool edge by an actuator controlled displacement of the complete tool in the micron-range. Small, periodic displacements applied perpendicular to the feed direction cause the trajectory to be changed to a short linear phase within the quality important sector of tool rotation (Fig. 2). This can be realized by active magnetic bearings or piezo-electric-actuators.

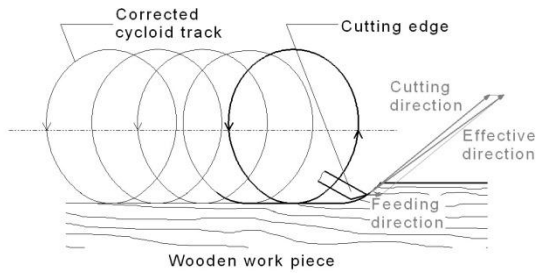


Figure 2. Avoiding of cutter-marks because of the corrected cycloid track of cutting edge when peripheral milling of wood

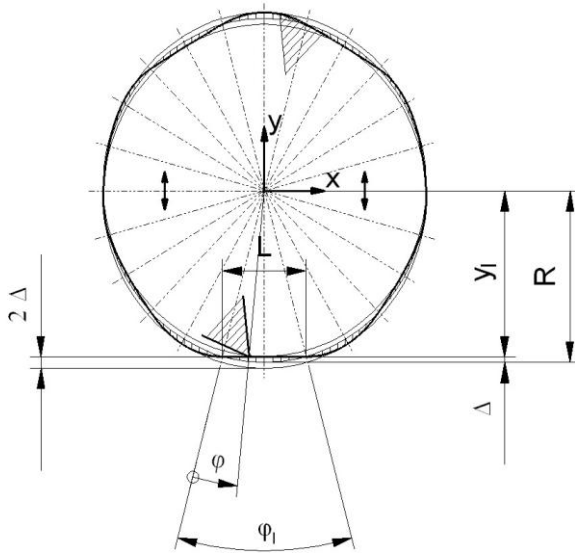


Figure 3. Visualisation of the periodic vertical cutting edge motion depending on the rotation angle φ of the tool to generate the linear movement with length L .

The actuators set the tool to periodic oscillation in the y -direction. The oscillations have to be synchronised to the rotational position of the cutting edge (Fig. 3). The angle of rotation of the rotor during which the cutting-edge is in contact with the work piece is called the rotation sector angle and is denoted by φ_1 . The period of tool axis oscillation is given by $2\varphi_1$, which is the double of the linearized/flattened rotation sector. The amplitude Δ can be calculated by (1) depending on the tool radius R and the linearized rotation sector angle φ_1 . The frequency of oscillation must be an integer multiple of the tool rotation number.

$$\Delta = R - y_l = R \cdot \left[1 - \cos\left(\frac{\varphi_1}{2}\right) \right]. \quad (1)$$

Furthermore, one has η as the displacement of the spindle axis in y -direction. Thus, (2) and (3) describe the two half periods of actuation in y -direction functionally depending on rotation angle φ , linearized rotation sector angle φ_1 and tool diameter R .

For $0^\circ \leq \varphi < \varphi_1$:

$$\eta(\varphi) = R \cdot \left[\cos\left(\frac{\varphi_1}{2} - \varphi\right) - \cos\left(\frac{\varphi_1}{2}\right) \right]. \quad (2)$$

For $\varphi_1 \leq \varphi \leq 2\varphi_1$:

$$\eta(\varphi) = -R \cdot \left[\cos\left(\frac{3 \cdot \varphi_1}{2} - \varphi\right) - \cos\left(\frac{\varphi_1}{2}\right) \right]. \quad (3)$$

The trajectory, along with the desired velocity and acceleration, is shown in Fig. 4. It should be noted that the velocity and acceleration plots have been rescaled. It can be seen that even though the desired velocity is continuous, the desired acceleration is not.

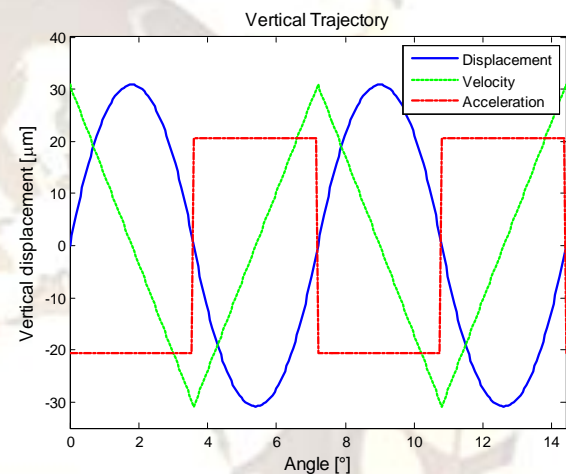


Figure 4: Desired trajectory of the spindle shown with (scaled) velocity and acceleration

A similar mechanism with a few piezo-electric actuators on a spindle ball bearing of a wood milling machine setup was already used and applied successfully for quality improvements some years ago by Hynek et al. [3, 4] and Jackson et al. [5]. In their case the front bearing was moved both in x - and y -direction for control of the cutting motion and reduction of the cutter-mark height.

The introduced solution approach and the following innovation shall improve the work piece quality and reduce the necessary finishing activities after milling. The changed process and the possibility to reduce the cutter-marks ought to lead to the chance to lower the very high rotational speeds of wood milling tools. Also, reduced rotation numbers and cutting speeds positively influence the cutting noise as well as tool wear.

III. PRELIMINARY EXPERIMENTS

3.1 Design Considerations

The periodic displacement of the tool is based on a tool diameter of 125 mm resulting in a tool radius $R = 62.5 \text{ mm}$. We use the ratio $N = 50$ between the oscillation frequency in the y-direction and the revolution frequency. This yields a linearized rotation sector

$$\varphi_l = \frac{360^\circ}{2 \cdot N} = \frac{180^\circ}{N} = 3.6^\circ.$$

The length L of the linear movement is given by

$$L = 2 \cdot R \cdot \sin\left(\frac{\varphi_l}{2}\right) \approx 3.93 \text{ mm}.$$

The amplitude Δ can be calculated by (1) as follows:

$$\Delta \approx 30.84 \mu\text{m}.$$

Since the tool axis oscillation is symmetric for both half periods as described by (2) and (3), actuators and measurement tools must be selected for a minimum range of $2\Delta \approx 62 \mu\text{m}$.

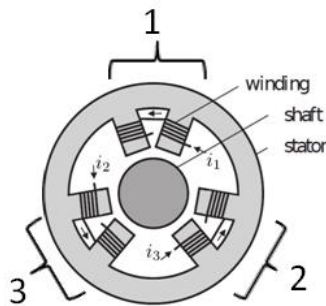


Figure 5: Radial bearing consisting of three horseshoe magnets

3.2 Experimental Setup

The spindle consists of a rotor of length 0.6 m and mass of 10 kg which is levitated by two three-phase electromagnetic radial bearings. Each of these radial bearings consists of three horseshoe magnets, arranged around the rotor at an effective angle of 120° to each other (see Fig. 5). Axial motion is controlled by a standard axial disc bearing. A laboratory spindle is shown in Fig. 6.

The power amplifiers used in the laboratory spindle are switched transistor bridges. The duty ratios of these transistor bridges can be used as the eight independent controls needed, namely, three for each radial bearing and two for the axial bearing. In industrial applications, current controlled amplifiers are widely used but in our setup current control is done by a cascaded controller, which is discussed in the next section. In our test-bench, the computer hardware used is dSpace 1103.

3.3 Mathematical Modeling

Modeling and controller design is described in [6, 7]. The cartesian coordinate system is set up as follows: x, y, z are the coordinates of the centre of mass of the rotor. The axis of symmetry of the rotor is also the axis of rotation and it coincides with the z -axis. The y -axis represents vertical displacement and the x -axis represents horizontal displacement. Since the rotor rotates about the z -axis with a constant angular velocity, both the rotation about the z -axis and displacement in the z -axis do not have to be considered. The angles ψ and θ describe the angular position of the rotor and ϕ is the angle of rotation, see Fig. 7.

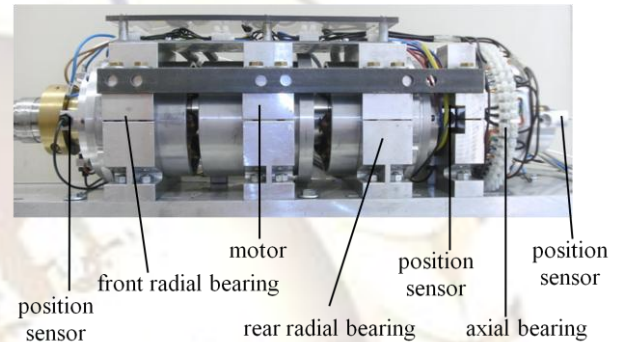


Figure 6: Laboratory spindle

Out of the six degrees of freedom of the rigid body, only four are considered. With these assumptions, the model can be written as [6]

$$\begin{aligned} m\ddot{x} &= F_{x,f} + F_{x,r} + mg_x \\ m\ddot{y} &= F_{y,f} + F_{y,r} + mg_y \\ J_2\ddot{\psi} &= -(l_f - z)F_{x,f} + (l_r - z)F_{x,r} - J_1\dot{\phi}\dot{\theta} \\ J_2\ddot{\theta} &= (l_f - z)F_{y,f} - (l_r - z)F_{y,r} - J_1\dot{\phi}\dot{\psi}, \end{aligned}$$

where l_f and l_r are the distances from the centre of mass of the rotor to the front and rear bearing, respectively. The mass of the rotor is denoted by m and J_1, J_2 are the principal moments of inertia. The forces in the x - and y -direction are denoted by F_x and F_y , and the indices r and f represent rear and front, respectively. The components of the gravitational acceleration are denoted by g_x, g_y and g_z . In case of appropriate adjustment we have $g_x = g_z = 0$ and $g_y = -g = -9.81 \text{ ms}^{-2}$. Since the axial displacement is small and the gyroscopic forces can be neglected, the model can be re-written as

$$\begin{pmatrix} \ddot{x} \\ \ddot{y} \\ \ddot{\psi} \\ \ddot{\theta} \end{pmatrix} = M \cdot \begin{pmatrix} F_{x,f} \\ F_{y,f} \\ F_{x,r} \\ F_{y,r} \end{pmatrix} + \begin{pmatrix} 0 \\ -g \\ 0 \\ 0 \end{pmatrix} \quad (4)$$

with

$$M = \begin{pmatrix} 1/m & 0 & 1/m & 0 \\ 0 & 1/m & 0 & 1/m \\ -l_f/J_2 & 0 & l_r/J_2 & 0 \\ 0 & l_f/J_2 & 0 & -l_r/J_2 \end{pmatrix}$$

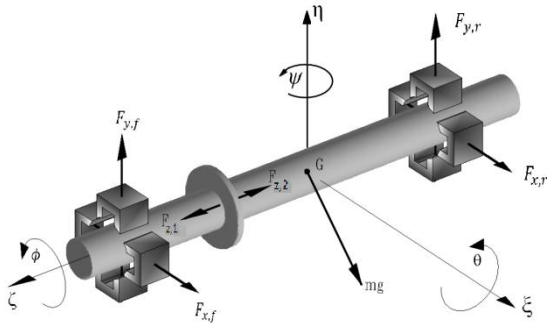


Figure 7: Magnetically levitated spindle

As can be seen in Fig. 5, the resulting force in each bearing is the sum of three independent forces created due to three currents in the horseshoe magnets. The forces in the front bearing can be represented by

$$\begin{pmatrix} F_{x,f} \\ F_{y,f} \end{pmatrix} = \begin{pmatrix} \sin(\alpha_1) & \sin(\alpha_2) & \sin(\alpha_3) \\ \cos(\alpha_1) & \cos(\alpha_2) & \cos(\alpha_3) \end{pmatrix} \begin{pmatrix} F_{1,f} \\ F_{2,f} \\ F_{3,f} \end{pmatrix}, \quad (5)$$

where $\alpha_1 = 0^\circ$, $\alpha_2 = 120^\circ$ and $\alpha_3 = 240^\circ$ and $F_{1,f}$, $F_{2,f}$ and $F_{3,f}$ are the forces generated by the horseshoe magnets. The forces in the rear bearing can be represented similarly.

The relationship between the current and the force is given by [6]

$$F_{i,j} = \mu_{i,j} \frac{i_{i,j}^2}{\left(s_j - (\sin \alpha_i \cos \alpha_i) \begin{pmatrix} x_j \\ y_j \end{pmatrix}\right)^2} \quad (6)$$

$$= \mu_{i,j} \frac{i_{i,j}^2}{(s_j - x_j \sin \alpha_i - y_j \cos \alpha_i)^2},$$

where $i \in \{1,2,3\}$ and $j \in \{f,r\}$, i is the current, s is the air gap and μ is a constant which depends on the bearing geometry and material. This simplified model neglects the interaction of the currents in different coils, saturation, and other nonlinear effects. The relationship given by (6) can be used to calculate the force inputs which serve as the controls of a flatness-based position tracking controller.

The current coils for each of the independent horseshoe magnets may be modeled as [6]

$$\frac{d}{dt}(Li) = u - Ri,$$

where R is the resistance of the coil, i is the current, u is the input voltage and L is the inductance which depends on position of the rotor.

Rotor angular position about the z -axis is measured with a contact-free incremental sensor. Rotor position and orientation is measured with two pairs of eddy current sensors in two planes perpendicular to the axis of symmetry and another one for the axial rotor position. The angular position is needed to synchronize the tool path with rotor rotation and the rotor position and orientation is needed for trajectory control.

3.4 Controller Design

The rigid body model (4) is used for the controller design [8]. The controller itself is flatness-based and has a cascade structure. The inner controller is used to follow the reference currents which are calculated by the outer loop, the position or tracking controller, which is shown in Fig. 8.

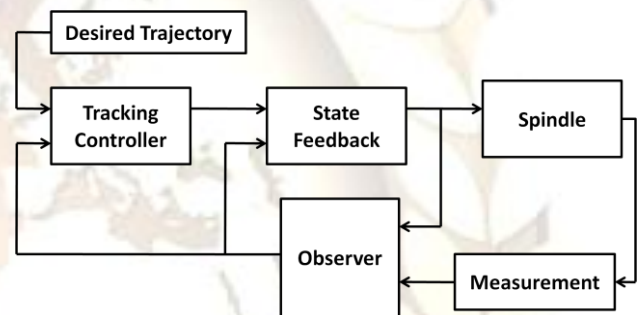


Figure 8. Signal flow diagram of the feedback control system.

The concept of flatness extends the concept of controllability from a linear system to a nonlinear system [9, 10]. Flatness based control requires the declaration of flat outputs, such that all states and inputs can be defined as a function of the flat outputs and their time derivatives. If such outputs can be found, then the system is said to be flat and these outputs can be used to determine the inputs needed to control the system. A major advantage of flatness based control is that integration is not required. For the purposes of the current problem, the position and orientation of the rotor can be selected as the flat outputs.

Defining a_x , a_y , a_ψ , a_θ as auxiliary variables, we have

$$\begin{pmatrix} a_x \\ a_y \\ a_\psi \\ a_\theta \end{pmatrix} = \begin{pmatrix} \ddot{x} \\ \ddot{y} \\ \ddot{\psi} \\ \ddot{\theta} \end{pmatrix}.$$

For each of the four uncoupled systems a stable controller can be designed. The desired or reference trajectory coordinates are denoted by x^{ref} , y^{ref} ,

ψ^{ref}, θ^{ref} . For example, for the displacement in the x direction we get

$$a_x = \ddot{x}^{ref} + (\lambda_{x,1} + \lambda_{x,2})(\dot{x} - \dot{x}^{ref}) - \lambda_{x,1}\lambda_{x,2}(x - x^{ref}).$$

Choosing the eigenvalues of the dynamics of the tracking error $\lambda_{x,1}$ and $\lambda_{x,2}$ so that they are symmetric about the real axis and in the open left side of the complex plane, a stable system is attained. Defining $e_x := x - x^{ref}$, the following equation is obtained:

$$\ddot{e}_x = (\lambda_{x,1} + \lambda_{x,2})\dot{e}_x - \lambda_{x,1}\lambda_{x,2}e_x.$$

Similarly, the tracking error may be defined as

$$e = \begin{pmatrix} e_x \\ e_y \\ e_\psi \\ e_\theta \end{pmatrix} = \begin{pmatrix} x^{ref} \\ y^{ref} \\ \psi^{ref} \\ \theta^{ref} \end{pmatrix} - \begin{pmatrix} x \\ y \\ \psi \\ \theta \end{pmatrix}, \quad (7)$$

where x and y are the position coordinates of the rotor and ψ and θ are the orientation angles of the rotor. The error dynamics are chosen so that they are decoupled linear oscillators:

$$\ddot{e} + K_1\dot{e} + K_0e = 0, \quad (8)$$

where K_0 and K_1 are diagonal matrices with real positive entries. We get

$$\begin{pmatrix} a_x \\ a_y \\ a_\psi \\ a_\theta \end{pmatrix} = \begin{pmatrix} \ddot{x} \\ \ddot{y} \\ \ddot{\psi} \\ \ddot{\theta} \end{pmatrix} = \begin{pmatrix} \ddot{x}^{ref} \\ \ddot{y}^{ref} \\ \ddot{\psi}^{ref} \\ \ddot{\theta}^{ref} \end{pmatrix} + K_1\dot{e} + K_0e.$$

Then the corresponding forces can be obtained from the rigid body model (4):

$$\begin{pmatrix} F_{x,f} \\ F_{y,f} \\ F_{x,r} \\ F_{y,r} \end{pmatrix} = M^{-1} \cdot \left(\begin{pmatrix} a_x \\ a_y \\ a_\psi \\ a_\theta \end{pmatrix} - \begin{pmatrix} g_x \\ g_y \\ 0 \\ 0 \end{pmatrix} \right) \quad (9)$$

$$= M^{-1} \cdot \begin{pmatrix} a_x \\ a_y + g \\ a_\psi \\ a_\theta \end{pmatrix}.$$

A crucial point of the experimental setup was the implementation of a nonlinear controller. A flatness-based controller design methodology was used. In general, nonlinear controller design can result in complicated symbolic expressions. As an alternative

to symbolic computation, one can employ algorithmic or automatic differentiation [11, 12]. As reported in [13], this approach has been successfully applied in nonlinear controller design for magnetic bearings.

3.5 Calculating the Control Current

Once the forces in (9) are obtained, the required currents in each horseshoe magnet must be calculated. For each bearing, there is no unique combination of currents which can be used to achieve the desired force. Therefore, one force must be chosen arbitrarily. Taking

$$F_{1,j} = \begin{cases} F_{0,j} & \text{if } F_{y,j} \leq -\frac{|F_{x,j}|}{\sqrt{3}} \\ F_{0,j} + F_{y,j} + \frac{|F_{x,j}|}{\sqrt{3}} & \text{otherwise,} \end{cases}$$

where $F_{0,j}$ is some arbitrary non-negative value and $j \in \{f, r\}$. The other forces can be obtained using the following:

$$F_{2,j} = F_{1,j} - F_{y,j} - \frac{F_{x,j}}{\sqrt{3}}$$

$$F_{3,j} = F_{1,j} - F_{y,j} + \frac{F_{x,j}}{\sqrt{3}}.$$

3.6 Experimental Results

Initial experiments were performed with the rotor turning at 110 rpm. Since $\varphi_l = 3.6^\circ$, the rotor makes one complete vertical oscillation for every 7.2° change in rotational angle. This leads to a frequency of the vertical oscillation of 91.67 Hz.

For a cutter-head with only two cutting edges the vertical trajectory of the spindle needs to be adjusted twice for each revolution of the rotor. If the cutting edge starts cutting at $\varphi_l = 0$ then the cutting takes place for $0 \leq \varphi \leq \varphi_l$ and $180^\circ \leq \varphi \leq 180^\circ + \varphi_l$. Therefore, it makes sense to reduce the amplitude of the vertical oscillations when the cutter edges are not in contact with the wood. The damping function is chosen to be

$$D(\varphi) = \left(\frac{\varphi - \frac{180^\circ + \varphi_l}{2}}{\frac{180^\circ - \varphi_l}{2}} \right)^8$$

for $\varphi_l \leq \varphi \leq 180^\circ$.

Fig. 9 shows the desired vertical displacement required along with the actual vertical displacement achieved. An over-shoot is clearly observed along with a delay/phase-angle. It should be clarified once again that the cutting only takes place when there is no damping, that is, when the angle is between 0° and 3.6°.

Fig. 10 shows the desired trajectory of the cutting-edge. Without any vertical movement the cutting edge would follow the circle. With vertical movement, ideally the cutting-edge should follow

the horizontal dashed line. It can be clearly seen that the overshoot from Fig. 9 leads to the cutting edge following a slightly higher trajectory than required. Nevertheless, the reduction in the groove formed is significant.

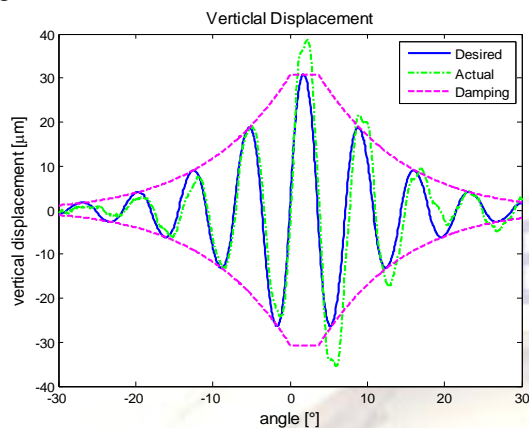


Figure 9: Plot of the desired and actual vertical displacement of the rotor

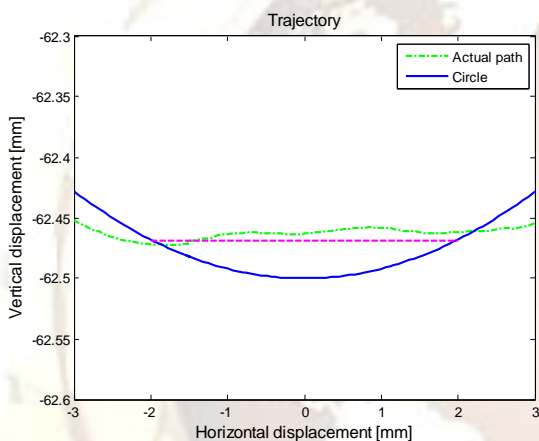


Figure 10: Trajectory of the cutting-edge (scaled)

IV. CONCLUSIONS

Wood milling procedures produce specific quality related surface patterns on the work piece called cutter-marks. This is because of the kinematical relations when milling and appears more or less depending on different cutting parameters. To improve this situation the cutting motion of the tool edge could be corrected by an periodic actuator controlled displacement of the complete tool in a micron-range to a linear motion.

The results show that significant improvement is achieved but there is room for further improvement. Specifically, the overshoot and the delay can be eliminated with a different controller design. Also, the reference trajectory may be changed to reduce or eliminate the vertical oscillations during the non-cutting phase. In addition, a reference trajectory can be chosen so that the required acceleration is not discontinuous. The results will be presented in upcoming publications.

ACKNOWLEDGEMENT

The authors would like to thank Dr. Jan Winkler and Dipl.-Ing. Christian John for their help and support.

REFERENCES

- [1] A. Wagenführ and F. Scholz (Ed.), *Taschenbuch der Holztechnik*. Leipzig: Fachbuchverlag im Carl Hanser Verlag, 2012.
- [2] G. Maier, *Holzspanungslehre*. Würzburg: Vogel Buchverlag, 2000.
- [3] P. Hynek, *Wood Surface Form Improvement by Real Time Displacement of Tool Trajectory*, PhD Thesis, Loughborough University, 2004.
- [4] P. Hynek, M. R. Jackson, R. Parkin, and N. Brown, "Improving wood surface form by modification of the rotary machining process", in *Proceedings of the Institution of Mechanical Engineers, Part B, Journal of Engineering Manufacture*, vol. 218, pp. 875-887, 2004.
- [5] M. R. Jackson, P. Hynek, and R. M. Parkin, "Active Timber machining: From Theory to Reality, in *Proceedings of 50. Internationales Wissenschaftliches Kolloquium*, TU Ilmenau (Germany), 19-23 September, 2005.
- [6] S. Eckhardt and J. Rudolph, *High Precision Synchronous Tool Path Tracking with an AMB Machine Tool Spindle*, in Ninth International Symposium on Magnetic Bearings, Lexington Kentucky, USA, 3-6 August, 2004.
- [7] J. Rudolph, F. Woittennek, and J. v. Löwis, *Zur Regelung eine elektromagnetische gelagerten Spindel*. at- Automatisierungstechnik, vol. 48, no. 3, pp. 132-139, 2000.
- [8] J. Levin, J. Lottin, and J. C. Ponsart, A nonlinear approach to the control of magnetic bearings. *IEEE Trans. Control Systems Technology*, vol 4, no. 5, pp. 524-544, 1996.
- [9] M. Fliess, J. L. Lévine, P. Martin, and P. Rouchon, Flatness and defect of non-linear systems: introductory theory and examples. *International Journal of Control*, vol. 61, no. 6, pp. 1327-1361, 1995.
- [10] R. Rothfuss, J. Rudolph, and M. Zeitz, Flachheit: Ein neuer Zugang zur Steuerung und Regelung nichtlinearer Systeme. at - Automatisierungstechnik, vol. 45, no. 11, pp. 517-525, 1997.
- [11] K. Röbenack and K. J. Reinschke, Reglerentwurf mit Hilfe des Automatischen Differenzierens at - Automatisierungstechnik, vol. 48, pp. 60-66, 2000.
- [12] K. Röbenack, Automatic Differentiation and Nonlinear Controller Design by Exact Linearization. *Future Generation Computer Systems*, vol. 21, pp. 1372-1379, 2005.
- [13] S. Palis, M. Stamann, and T. Schallschmidt, Nonlinear control design for magnetic bearings via automatic differentiation, in *Proc. 13th Power Electronics and Motion Control Conference*, pp. 1660 - 1664, 2008.